Journal of Thermal Engineering
Yildiz Technical University Press, Istanbul, Turkey
Vol. 1, Special Issue 1, pp. 192-202, February, 2015.

http://eds.yildiz.edu.tr/journal-of-thermal-engineering/Articles
Manuscript Received September 26, 2014; Accepted October 20, 2014

This paper was recommended for publication in revised form by Regional Editor Bekir Sami Yılbaş

EXERGY-BASED THERMODYNAMIC ANALYSIS OF SOLAR DRIVEN ORGANIC RANKINE CYCLE

***Esa Dube Kerme**
Sustainable Energy Technologies Center
College of Engineering
King Saud University
P.O.BOX800, Riyadh 11421, Saudi Arabia

Jamel Orfi
Departments of Mechanical Engineering
College of Engineering
King Saud University
P.O.BOX800, Riyadh 11421, Saudi Arabia

Key words: Parabolic trough solar collectors, organic Rankine cycle, exergetic efficiency,exergy destruction rate, irreversibility ratio

*Corresponding Author: Esa Dube Kerme
E-mail: esadube@gmail.com

ABSTRACT

In this paper thermodynamic modeling of organic Rankine cycle (ORC) driven by parabolic trough solar collectors is presented. Eight working fluids for the ORC were examined. The effect of turbine inlet temperature on main energetic and exergetic performance parameters were studied. The influences of turbine inlet temperature on turbine size parameter, turbine outlet volume flow rate and expansion ratio were also investigated. Important exergetic parameters including irreversibility ratio and total exergy destruction rate were also included in the analysis and evaluated. The study reveals that increasing the turbine inlet temperature results in increasing the net electric efficiency, net power output, exergy efficiency and expansion ratio while the total exergy destruction rate and turbine size parameter are reduced. From the considered working fluids, o-xylene gives the best energetic and exergetic performance. The results of the study also show that the main source of exergy destruction occurs in the solar collector where 74.9% of the total exergy loss is destructed. Next to collectors, 18.2% of the total destructed exergy occurs in the condenser.

1. INTRODUCTION

The use of solar energy as a primary source for power generation has become crucial and is expected to increase in the near future. This is due to the fact that utilization of solar energy systems offer better advantages over electricity generation using conventional energy sources. These benefits fall into two main categories: environmental and socio-economic issues. From an environmental point of view, the use of solar energy technologies has several positive implications that include: reduction of the emission of greenhouse gases (mainly CO_2, NO_x) and of toxic gas emissions (SO_2, particulates), recovery of degraded land, reduced requirement for transmission lines within the electricity grid and improvement in the quality of water resources [1-3, 5-7]. The socio-economic benefits of solar technologies include: increased regional and national energy independence, creation of employment opportunities [4,5], and acceleration of electrification of rural communities in isolated areas and diversification and security (stability) of energy supply [2-4]. Overall, since solar energy is an inexhaustible, clean and safe source of energy, it has received much attention as one of the most promising candidate to substitute the conventional sources (fuels) for energy supply [8-10].

Organic Rankine cycle (ORC) as a promising energy conversion technology has been the focus of many researches in recent years due to its typical advantages of using low grade heat source, such as industrial waste heat, solar energy and geothermal energy. Many investigators have considered the thermodynamic analysis and optimization of ORC to enhance its performance. Wei et al [11] studied effects of parameters such as exhaust mass flow rate, exhaust inlet temperature, air mass flow rate, and ambient temperature on the net power output, system efficiency and exergy destruction rate of ORC for waste heat recovery. They obtained that choosing appropriate nominal state was a good idea to improve the system net power output and efficiency. Roy and Misra [12] conducted thermodynamic parametric study of an ORC using R-123 by considering intermediate heat source temperature. They found that the best thermodynamic performance of the cycle can be obtained at a turbine inlet pressure of 2.7 MPa. Besides, several other authors including Quoilin et al. [13], Nguyen et al., Saitoh et al. [14], Kane et al. [15] and Yagoub et al. [16] proposed and studied different micro-ORCs designed for electricity generation.

A number of papers had investigated the utilization of solar energy as a primary source for power production (electricity generation) integrating with ORC. He et al. [17], for example, numerically simulated parabolic trough solar power generation system integrated with organic Rankine cycle in order to study the effects of various key parameters on collector field and system performance. Quoilin et al. [18] presented the design and characteristics of a small scale, low cost solar-powered ORC for rural electrification. They developed a model, compared several working fluids and optimized the working conditions of the system. Tchanche et al.[19] made comparative assessment of some working fluids that are used in low-temperature solar organic Rankine cycle systems with regard to their performances as well as thermodynamic and environmental properties. They used efficiencies, volume flow rate, mass flow rate, pressure ratio, toxicity, flammability, ozone depletion potential and global warming potential for comparison. They found that among the investigated fluids, R134a is the most suitable working fluid of ORC for small scale solar applications.

In a different study, a low temperature solar thermal electric system with regenerative ORC and compound parabolic concentrator was investigated by Pei et al. [20].The heat transfer and power conversion processes were simulated, and the effects of the regenerative cycle on the collector, ORC, and overall electric efficiencies were analyzed. Their simulation results showed that the maximum regenerative ORC efficiency and overall system efficiency are higher than without the regenerative cycle by 9.2% and 4 to 5.4% respectively. They concluded that low temperature solar thermal power generation which is a modular technology is promising. In addition, Li et al. [21] proposed a novel design of solar thermal power generation system consisting of compound parabolic concentrators (CPC) and organic Rankine cycle (ORC) working with HCFC-123. They investigated influences of collector tilt angle adjustment, connection between heat exchangers and the CPC collectors, and ORC evaporation temperature on the overall system performance. Their results indicated that the annual received direct irradiance, number of stages of collectors and ORC evaporation temperatures are the three factors which have a major impact on the annual electricity output and should be the key points of optimization.

In another paper, Wang et al. [22] studied a regenerative organic Rankine cycle to utilize the solar energy over a low temperature range using flat plate solar collectors. They conducted parametric analysis in order to examine the effects of turbine inlet temperature, turbine inlet pressure and condensation temperature on the system performance using different working fluids. Their study indicated that increasing turbine inlet pressure and temperature or lowering the turbine back pressure could improve system performance. They also found that among the evaluated working fluids, R245fa and R123 are the most suitable working fluids for the system due to their high system performance and low operation pressure. Fahad A. Al-Suleiman [23] studied, energy and sizing analyses of parabolic trough solar collector integrated with steam and binary vapor cycles. He examined seven refrigerants (R600, R600a, R134a, R152a, R290, R407c and Ammonia) for ORC as bottoming cycle. His study revealed that R134a binary vapor cycle has the best performance among the binary vapor cycles considered and requires the smallest solar field size while the R600a binary vapor cycle has the lowest performance.

It can be seen from the literature review that there are few studies of energy and exergy analysis that have been conducted on organic Rankine cycle integrated with parabolic trough solar collectors for power generation. The detail studies of energy and exergy analysis that have been conducted on organic Rankine cycle with high critical temperature working fluid (i.e. o-xylene as a working fluid) confirms the originality and the role of the work in this paper.

The aim of this study is to conduct energetic and exergetic performance analysis of organic Rankine cycle driven by solar energy received by parabolic trough solar collectors. As a working fluid of ORC, eight organic fluids have been considered including: o-xylene, ethylbenzene, toluene, n-octane, n-nonane, n-heptane, dimethylcarbonate (DMC) and benzene. Furthermore, the effect of turbine inlet temperature and condenser temperature on key energetic and exergetic performance parameters are examined. In addition, the variation of turbine size parameter, turbine outlet volume flow rate and expansion ratio with turbine inlet temperature are studied. Detailed exergy parameters including irreversibility ratio, improvement potential and fuel depletion ratio are also analyzed.

2. SYSTEM DESCRIPTION

The solar driven organic Rankine cycle system consists of a solar energy collecting subsystem and an organic Rankine cycle subsystem. Fig.1 illustrates the schematic diagram of the entire system. The organic Rankine cycle subsystem consists of four main components, namely: an evaporator, a turbine, a condenser and a pump. The ORC is integrated with the parabolic trough collector solar field through the evaporator. The liquid organic working fluid from condenser is compressed by the pump and fed back to the evaporator, where it is heated by the useful heat delivered by the solar PTC collectors,

becomes superheated vapor. The superheated vapor enters the turbine and expands to a low pressure to produce electricity by rotating the shaft connected to an electric generator. Afterwards, the turbine exhaust is condensed to liquid in the condenser by rejecting heat to the environment and the cycle completes when the fluid is compressed by the pump.
The major part of solar energy collecting system is an array of solar collector field made of parabolic trough solar collector modules. The length of each module is 14 m [24]. The receiver is the pipe carrying the heat transfer fluid. Outside this receiver is vacuum annulus to reduce heat losses. The geometric data of the solar collectors are given in Table 1. The type of the collector selected is Sky Trough collector. The heat transfer fluid selected for the solar loop is Therminol-VP1. This oil has been selected based on the fact that it has better heat transfer properties and temperature control [26], and, hence, it is used in many different power plants driven by parabolic trough collectors, [26, 27]. The characteristics of this fluid can be found at [26].

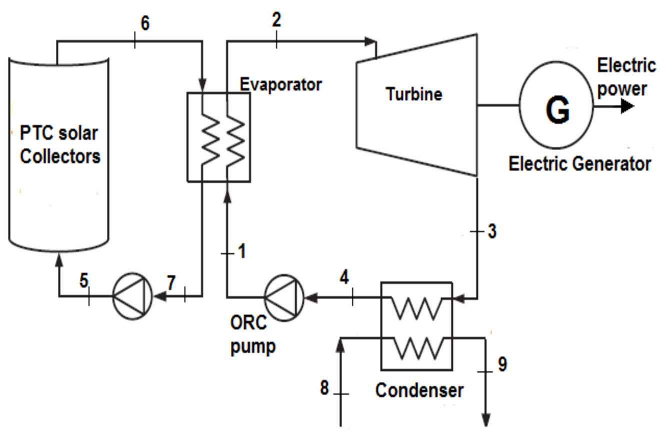

FIGURE 1. SCHEMATIC DIAGRAM OF ORGANIC RANKINE CYCLE INTEGRATED WITH PARABOLIC TROUGH SOLAR COLLECTORS

3. MATHEMATICAL MODELING

The solar driven ORC for power generation is mathematically modeled using mass, energy and exergy balances on each component as well as on the whole system. To simplify the theoretical analysis, some assumptions are made as follows:

(i) The system runs at steady state process
(ii) Pressure drop and heat loss in pipelines are all neglected. Pressure losses in pump and turbine are however included in the model.
(iii) The working fluid at the condenser outlet (pump inlet) is saturated liquid.
(iv) Kinetic and potential energy and exergy are ignored.
(v) Chemical exergy of materials is neglected.
(vi) The dead state properties are taken as T_o = 25 °C and P_o =101.325 kPa.

3.1 ENERGY ANALYSIS

3.1.1 SOLAR ENERGY COLLECTING SUBSYSTEM

Modeling of Parabolic trough collector solar subsystem is based on the equations presented in [28, 29]. The rate of useful energy delivered by single collector is defined as

$$Q_u = A_{ap} F_R \left(S - \frac{A_r}{A_{ap}} U_L (T_{fi} - T_a)\right) \tag{1}$$

where F_R is the heat removal factor, S is the heat absorbed by the receiver, A_{ap} is the aperture area, A_r is the receiver area, and U_L is the solar collector overall heat loss coefficient. The heat absorbed by the receiver is defined as:

$$S = G_b \eta_r \tag{2}$$

where G_b is the direct irradiation intensity and η_r is the receiver efficiency defined as:

$$\eta_r = \rho\gamma\tau\alpha K \tag{3}$$

where ρ,γ,τ,α and K are the reflectance of the mirror, intercept factor, transmittance of the glass cover, absorptance of the receiver and incidence angle modifier respectively and their values are given in table 1. The heat removal factor is given by
[28, 29]:

$$F_R = \frac{m_r Cp_r}{A_r U_L}\left[1 - \exp\left(-\frac{A_r U_L F_l}{m_r Cp_r}\right)\right]$$

(4)

where m_r is the mass flow rate through the receiver and F_l is the collector efficiency factor defined as:

$$F_l = \frac{1/U_L}{\dfrac{1}{U_L} + \dfrac{D_o}{D_i\, h_{fi}} + \dfrac{D_o}{2\,k}\ln\left(\dfrac{D_o}{D_i}\right)} \tag{5}$$

where k is the thermal conductivity of the receiver tube and h_{fi} is the convection heat transfer coefficient inside the receiver tube and it can be obtained from:

$$h_{fi} = \left(\frac{Nu\, k_{fi}}{D_i}\right) \tag{6}$$

where Nu is Nusselt number. As the flow inside the receiver tube is turbulent (i.e Re > 2300), Nusselt number can be evaluated using the following correlation [28]:

$$Nu = 0.023(\mathrm{Re})^{0.8}(\mathrm{Pr})^{0.4} \tag{7}$$

where Re is Reynolds number of the flow inside the receiver tube and Pr is the fluid Prandtl number.
The solar collector heat loss coefficient between ambient and receiver is defined as:

$$U_L = \left[\frac{A_r}{(h_{c,ca} + h_{r,ca})A_c} + \frac{1}{h_{r,cr}}\right]^{-1} \tag{8}$$

The radiation heat coefficient between ambient and the cover is given by:

$$h_{r,ca} = \varepsilon_c \sigma (T_c + T_a)(T_c^2 + T_a^2) \tag{9}$$

where σ is Stefan–Boltzmann constant and ε_c is the emittance of the cover. The radiation heat coefficient between the cover and the receiver is defined as:

$$h_{r,cr} = \sigma \frac{(T_c + T_r)(T_c^2 + T_r^2)}{1/\varepsilon_r + (A_r/A_c)(1/\varepsilon_c - 1)} \tag{10}$$

where T_r is receiver average temperature. The convection heat loss coefficient between ambient and the cover is defined as:

$$h_{c,ca} = \left(\frac{Nu k_{air}}{D_{co}}\right) \tag{11}$$

where k_{air} is the thermal conductivity of the air and Nu is Nusselt number. The cover temperature of the receiver is obtained by the equation:

$$T_c = \frac{A_r h_{r,cr} + A_c(h_{c,ca} + h_{r,ca})T_a}{A_r h_{r,cr} + A_c(h_{c,ca} + h_{r,ca})} \tag{12}$$

The total amount of solar radiation that shines up on the collector field, which is the total energy input to the system is defined as:

$$\dot{Q}_{solar} = A_{ap} F_R S N_t \tag{13}$$

where N_t is total number of collectors and A_{ap} is aperture area obtained as:

$$A_{ap} = (w - D_{co})L \tag{14}$$

where L, w, and D_{co} are the collector (module) length, width and receiver cover outer diameter respectively.

3.1.2 ORGANIC RANKINE CYCLE SUBSYSTEM

The organic Rankine cycle subsystem is modeled based on the laws of mass and energy conservation. In the evaporator, the heat addition into the power cycle is given by:

$$\dot{Q}_E = \dot{m}_f (h_2 - h_1) \tag{15}$$

In the condenser, heat rejected is expressed as:

$$\dot{Q}_C = \dot{m}_f (h_3 - h_4) \tag{16}$$

For the turbine, the isentropic efficiency is expressed as:

$$\eta_T = \frac{h_2 - h_3}{h_2 - h_{3s}} \tag{17}$$

The power output of the turbine is given by:

$$\dot{W}_T = \dot{m}_f (h_2 - h_3) \tag{18}$$

For the pump, the isentropic efficiency can be expressed as:

$$\eta_p = \frac{h_{1s} - h_4}{h_1 - h_4} \tag{19}$$

The ORC pump power consumption is defined as:

$$\dot{W}_p = \dot{m}_f (h_1 - h_4) \tag{20}$$

The net electric power generated by the solar driven ORC is defined as:

$$\dot{W}_{net,el} = \eta_g \dot{W}_T - \frac{\dot{W}_p}{\eta_{motor}} \tag{21}$$

Where η_g and η_{motor} are generator and motor efficiency respectively. The net electric efficiency of the system is defined as:

$$\eta_{el} = \dot{W}_{net,el} / \dot{Q}_{solar} \tag{22}$$

3.2 EXERGY ANALYSIS

Exergy analysis uses the first and second laws of thermodynamics and permits many of the shortcomings of energy analysis to overcome. It is useful in identifying the causes, locations, and magnitudes of process inefficiencies. Exergy is defined as the maximum theoretical work that can be attained from a system as it interacts with the equilibrium state (surroundings). The exergy balance of a control volume at steady state can be defined as [30]:

$$\sum \left(1 - \frac{T_o}{T_k}\right)\dot{Q}_k - \dot{W} + \sum_{in} \dot{m}\psi - \sum_{out} \dot{m}\psi - \dot{E}x_d = 0 \tag{23}$$

where $\dot{E}x_d$, ψ and T are the exergy destruction rate, exergy flow and temperature respectively. The subscript o is the value of the property at the surrounding and the subscript k is the property value at state k. The exergy destruction is an important parameter in exergy analysis. It is defined as the potential work lost due to irreversibility. The exergy destruction rate of a control volume at steady state can be obtained from equation 23. The physical flow exergy per unit mass flow is defined as [30]:

$$\psi = (h - h_o) - T_o(s - s_o) + \left(\frac{v^2 - V_o^2}{2}\right) + g(z - z_o) \tag{24}$$

where h, s, v, g, and z are enthalpy per unit mass, entropy per unit mass, velocity, gravity, and elevation, respectively. In this study, the elevation and velocity are neglected as they are significantly small as compared to the other values.The exergy efficiency is defined as the ratio of exergy recovered to the exergy input to the system. The net electrical exergy efficiency of the considered solar driven ORC system is defined as [30]:

$$\eta_{exergy,el} = \frac{\dot{W}_{net}}{\dot{E}x_{in}} \tag{25}$$

where $\dot{E}x_{in}$ is the inlet exergy to the system, and it is the function of the sun's outer surface temperature (T_s = 6000 K) and defined as [31]:

$$\dot{E}x_{,in} = A_{ap,total} G_b \left(1 + \frac{1}{3}\left(\frac{T_o}{T_s}\right)^4 - \frac{4}{3}\left(\frac{T_o}{T_s}\right)\right) \tag{26}$$

The irreversibility ratio of each component of solar driven ORC system is defined as [32]:

$$IR = \frac{\dot{E}xd}{\dot{E}xd_{,total}} \tag{27}$$

The turbine size parameter (SP) is another crucial parameter in studying the size character of the turbine in the organic Rankine cycle system. It is defined as [33]:

$$SP = \sqrt{\dot{V}_3} / \sqrt[4]{\Delta h} \tag{28}$$

where $\dot{V}_3$ is the volume flow rate of the working fluid at the outlet of the turbine and Δh is the specific enthalpy drop in the turbine.

The developed equations are programmed by using engineering equations solver (EES) [34]. In fact, EES provides numerical solution of nonlinear algebraic and differential equations. In addition, EES provides built-in thermodynamic and transport property functions for many fluids, including water, dry and moist air, organic fluids (refrigerants), and others. The input data used in the code are given in Table 1.

TABLE 1. INPUT DATA USED IN THE SYSTEM ANALYSIS

Organic Rankine Cycle (ORC)	**Value**
Isentropic turbine efficiency	85%
Isentropic pump efficiency	85%
Mass flow rate	4 kg/sec
Turbine inlet pressure	2MPa
Pump inlet temperature	120°C
PTC Solar collectors characteristics	
Aperture width	6m
PTC Length per module	14m
Receiver Inner diameter	0.08m
Receiver Outer diameter	0.0889m
Glass cover diameter	0.125m
Transmissivity of the receiver	0.94
Absorptivity of the receiver	0.97
Reflectivity of the aperture surface	0.96
Intercept angle	1
Receiver emittance	0.92
Glass cover emittance	0.87

4. VALIDATION OF THE MODEL

The validation of the ORC model is shown in Figure 2. It indicates the thermal efficiency of an ideal Rankine cycle, using R-123(HCFC-123) as working fluid, calculated by the present model and the results obtained by Madhawa Hettiarachchi et al. [35. It can be seen that there is a good agreement between the present results and those of Madhawa Hettiarachchi et al. [35] for the entire range of turbine inlet temperature.

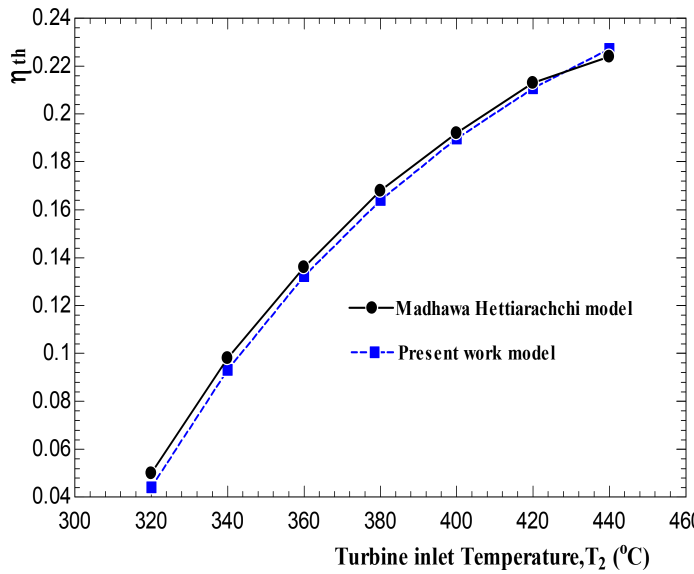

FIG. 2. VALIDATION OF THE ORC PRESENT MODEL WITH MADHAWA HETTIARACHCHI [35].THERMAL EFFICIENCY VERSUS TURBINE INLET TEMPERATURE FOR AN IDEAL RANKINE CYCLE USING R123 (HCFC-123) AND CONDENSER TEMPERATURE OF 303K.

TABLE 2. PROPERTIES OF THE SELECTED ORGANIC WORKING FLUIDS [34]

Working Fluids	**Type of Fluids**	**Molecul. Weight (g/mol)**	**T_{cr} (°C)**	**P_{cr} (kPa)**
O-xylene	Dry	106.2	357.1	3738
Toluene	Dry	92.14	318.6	4126
Ethylbenzene	Dry	106.2	344	3622
Benzene	Isentropic	78.11	288.9	4894
n-Octane	Dry	114.2	296.2	2497
n-Nonane	Dry	128.26	321.4	2281
n-Heptane	Dry	100.2	267	2727
Dimethyl Carbonate (DMC)	Dry	90.08	284.2	4909

TABLE 3. THERMODYNAMIC PROPERTIES OF EACH STATE FOR THE SOLAR DRIVEN ORC SYSTEM

No.	Fluid type	$\dot{m}$ (kg/s)	P (kPa)	T (°C)	h (kJ/kg)	ψ (kJ/kg
1	O-xylene	4	2000	121	294.2	26.33
2	O-xylene	4	2000	306.6	853.9	254
3	O-xylene	4	50.65	184.5	759.9	144.5
4	O-xylene	4	50.65	120	291.1	24.81
5	Therminol -VP1	5.5	199.1	130	199.1	25.54
6	Therminol -VP1	5.5	351.6	322.2	605.7	178.5
7	Therminol -VP1	5.5	198.9	129.9	198.9	25.5
8	Cooling water	11.2	101.3	25	104.8	0
9	Cooling water	11.2	101.3	65	272.1	10.33

5. RESULTS AND DISCUSSION

In this section, the numerical simulation of the solar driven organic Rankine cycle using the mathematical models established in section 3 will be presented. Riyadh city in the Kingdom of Saudi Arabia (24.72°N, 45°E) is selected as the case city. The analyses are performed for eight working fluids. Thermo-physical properties of these working fluids, as shown Table 2, are obtained by using engineering equation solver (EES).The input conditions used for the simulation are listed in Table 1. The effects of turbine inlet temperature on key selected overall system performance parameters are examined. The performance of the system was evaluated under the solar direct normal irradiation intensity, Gb = 0.47kW/m^2, as a minimum value in Riyadh city required for the operation of the system under consideration. The thermodynamic properties under the baseline conditions for the solar irradiation intensity of Gb = 0.470 kW/m^2 of the system considered in the study are listed in Table 3.The performance parameters include net electrical power output, net electrical efficiency, exergy efficiency, total exergy destruction rate, component's exergy destruction rate, turbine outlet volume flow rate, expansion ratio and turbine size parameter.

5.1 EFFECT OF TURBINE INLET TEMPERATURE ON THE SOLAR DRIVEN ORC SYSTEM

Due to the fact that turbine inlet temperature is significantly important in the design of solar driven ORC, it is being investigated in this study. Figs.3-7 illustrate the effect of turbine inlet temperature on performance of the system under consideration. Assuming that the condenser temperature is 120°C, Figs.3 and 4 respectively show that the net electric power output and electric efficiency increase with increasing turbine inlet temperature. These figures also illustrate that n-nonane, n-octane and n-heptane show small increase of power and efficiency with turbine inlet temperature. O-xylene is the organic fluid that provides the highest electric efficiency and the net electric power output among the selected working fluids.

Figs.5 and 6 illustrate the effect of turbine inlet temperature on the overall exergetic efficiency and total exergy destruction rate of the system respectively. Figure 5 indicates that in a fashion similar to the electric efficiency, the exergy efficiency of system increases with increasing turbine inlet temperature. One can note that exergy efficiency and destruction rates for the n-nonane, n-octane and n-heptane working fluids show small increment with the variation of the turbine inlet temperature. The situation is different for the other working fluids, where their respective performance is better at high turbine inlet temperature values. Besides, the total exergy destruction rate, as indicated in Fig. 6, decreases with increasing turbine inlet temperature. The organic fluid with best exergy efficiency is o-xylene, whereas the organic fluid with lowest exergy efficiency is n-heptane. O-xylene is the organic fluid with highest critical temperature, whereas n-heptane is the one with lowest critical temperature. Therefore, it gives the impression that organic fluid should be selected so that its critical temperature is closer to the output temperature of the heat transfer fluid of the solar collector. Based on the fact that o-xylene with critical temperature of 357.1°C gives the best exergetic performance, it has been selected as the working fluid of the system considered in this study.

Figure 7 presents the ORC component's and total exergy destruction rate as a function of turbine inlet temperature using o-xylene as a working fluid. It can be noticed from the figure that most of the exergy is destroyed by solar collectors and it decreases slightly as turbine inlet temperature increases. On the other hand, other components destroy less exergy. The condenser and pump exergy destruction rate increases while the turbine and evaporator exergy destruction rate decreases with increasing turbine inlet temperature.

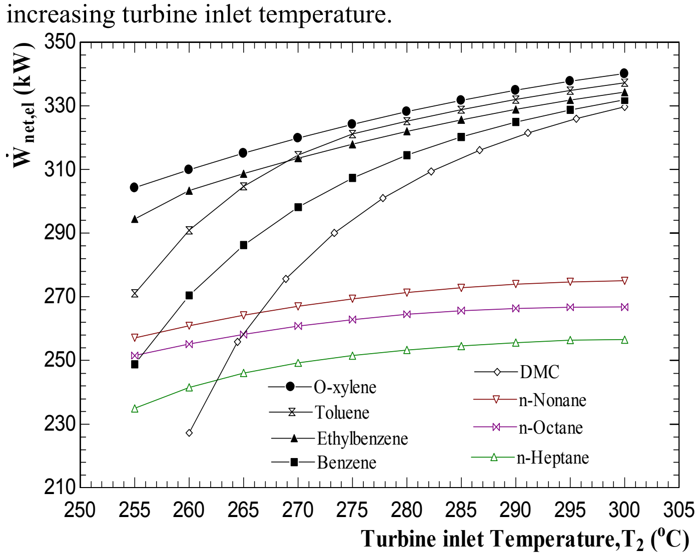

FIG. 3. VARIATION OF NET ELECTRICAL POWER OUTPUT WITH TURBINE INLET TEMPERATURE FOR VARIOUS ORGANIC WORKING FLUIDS AT CONDENSER TEMPERATURE (T_4) OF 120°C.

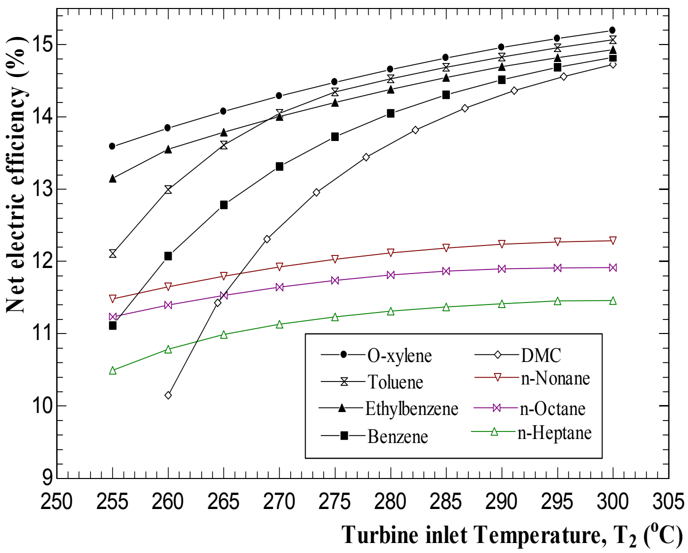

FIG. 4.VARIATION OF NET ELECTRIC EFFICIENCY WITH TURBINE INLET TEMPERATURE FOR VARIOUS ORGANIC WORKING FLUIDS AT CONDENSER TEMPERATURE OF 120^{O}C.

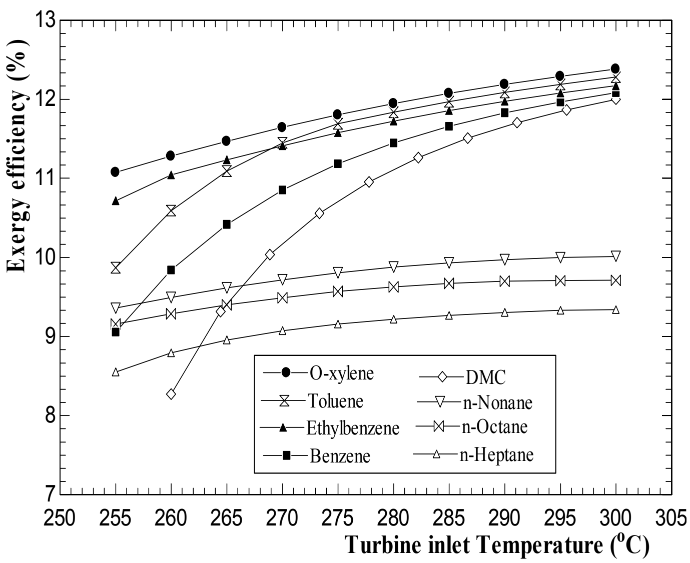

FIG.5.VARIATION OF EXERGY EFFICIENCY WITH TURBINE INLET TEMPERATURE FOR VARIOUS ORGANIC WORKING FLUIDS AT CONDENSER TEMPERATURE OF 120^{O}C.

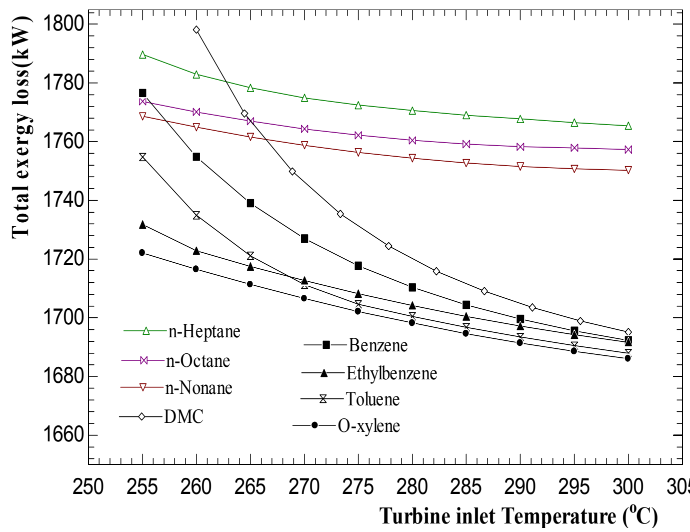

FIG. 6. VARIATION OF TOTAL EXERGY DESTRUCTION RATE WITH TURBINE INLET TEMPERATURE FOR VARIOUS ORGANIC WORKING FLUIDS AT CONDENSER TEMPERATURE OF 120^{O}C.

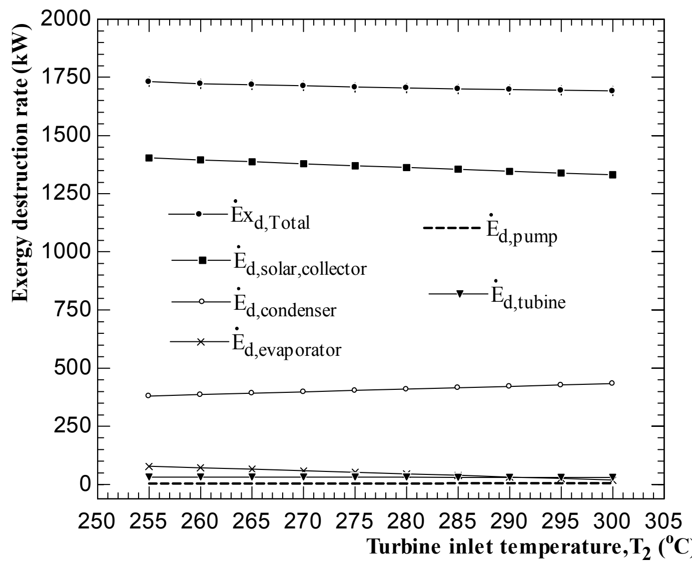

FIG. 7. VARIATION OF ORC COMPONENTS' EXERGY DESTRUCTION RATE WITH TURBINE INLET TEMPERATURE AT CONDENSER TEMPERATURE OF 120^{O}C

The volumetric flow rate is an important parameter in the organic Rankine cycle design, component sizing and system cost. The higher the volumetric flow rate (higher expansion ratio), the bigger the component size and the higher the work absorbed by the fluid circulation pump. Volumetric flow rate at turbine outlet together with expansion ratio give important information about expander design. Expansion ratio is the ratio of turbine outlet volume flow rate to that of its inlet volume flow rate. The variation of turbine outlet volume flow rate and expansion ratio with turbine inlet temperature is indicated in

Figs. 8 and 9 respectively. From the figures, it is seen that in general, the volume flow rate at the turbine exit exhibits small decreasing with an increment of temperature while expansion ratio increases with turbine inlet temperature for all working fluids. This shows that the inlet turbine volume flow rate is sensitive to temperature changes. Results of calculations in the Figures also show that n-nonane, n-octane, o-xylene and ethylbenzene have high volume flow rate and expansion ratio. Fluids with low volume flow rate and low expansion ratio are: n-Heptane, DMC (dimethyl carbonate) and benzene, and they are preferable for economic reasons.

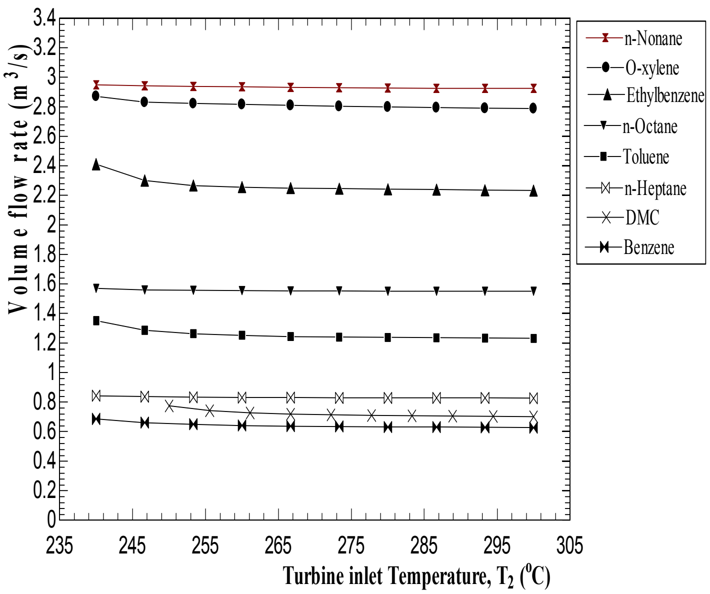

FIG. 8. TURBINE OUTLET VOLUME FLOW RATE VERSUS TURBINE INLET TEMPERATURE FOR VARIOUS ORGANIC WORKING FLUIDS AT CONDENSER TEMPERATURE OF 120^{O}C

Figure 10 illustrates the effect of the turbine inlet temperature on the turbine size parameter (SP) for various working fluids at condenser temperature of 120ºC. As the figure indicates, the turbine size parameter shows small decreasing with increasing turbine inlet temperature. At the same high turbine inlet temperature of 300ºC, small size parameters are obtained for benzene (0.2529m), DMC (dimethyl carbonate, 0.2691m), and n-heptane (0.3042m) while n-nonane requires the largest size parameter (0.5787m) of all working fluids.

The exergy analysis that was conducted through the exergetic assessment of the main components of the system under consideration is discussed in this section. The important exergy parameters considered in this exergetic assessment include: exergy destruction rate and irreversibility ratio as shown in Table 4. The values of these parameters are calculated under the baseline conditions: turbine inlet pressure of 2 MPa, condenser temperature of 120ºC and direct normal irradiance (DNI) of 470W/m^2.

From Table 4, it is seen that the total exergy destruction rate corresponding to the whole system reaches 1997 kW. Such irreversibility rates occur mainly in the solar collectors. It has been calculated that the exergy destructed in the solar collector is 1495 kW. The main cause for this large exergy destruction is the large temperature difference in the solar collector. Other main sources of exergy destruction occur in the condenser, the evaporator and the turbine with an exergy loss of 364.2kW, 68.92kW and 62.12 kW respectively. As indicated above, the main source of exergy destruction is the solar collector and, thus, it requires careful design to improve its performance. An improved design includes, mainly, higher optical efficiency of the solar collector and less heat losses from the receiver.

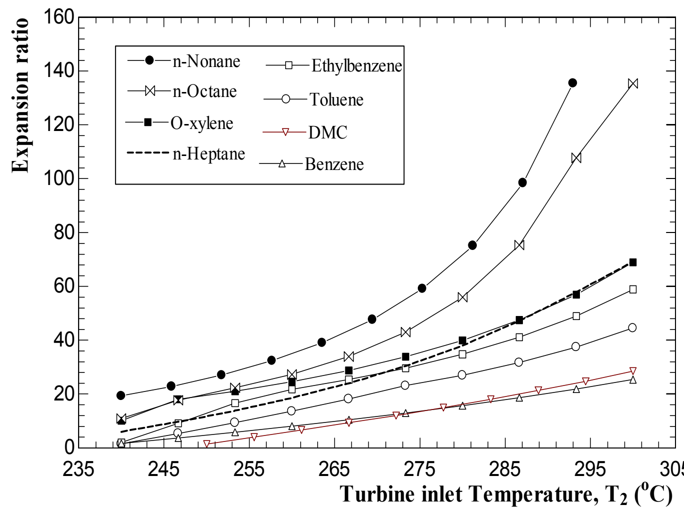

FIG. 9. EXPANSION RATIO VERSUS TURBINE INLET TEMPERATURE FOR VARIOUS WORKING FLUIDS AT CONDENSER TEMPERATURE OF 120^{O}C.

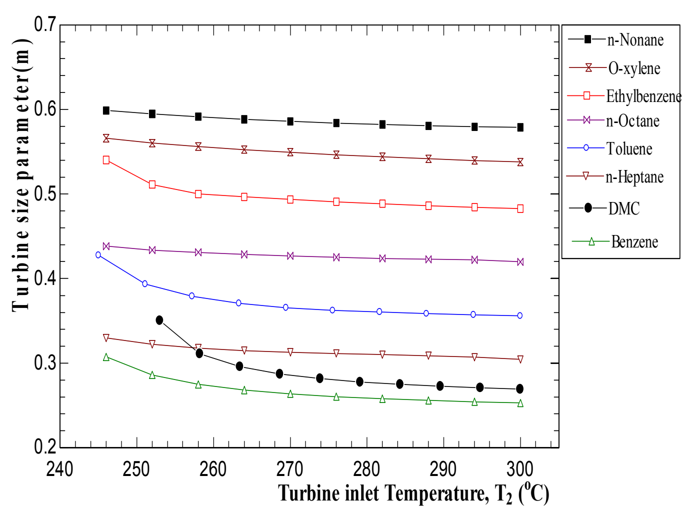

FIG. 10.VARIATION OF TURBINE SIZE PARAMETER WITH TURBINE INLET TEMPERATURE FOR DIFFERENT WORKING FLUIDS AT CONDENSER TEMPERATURE OF 120^{O}C

TABLE 4. DETAILED EXERGY PARAMETERS FOR SOLAR DRIVEN ORC USING O-XYLENE AS A WORKING FLUID

Components	Exergy destruction (kW)	Irreversibility ratio
Solar collector	1495	0.749
Evaporator	68.92	0.035
Turbine	62.12	0.031
Condenser	364.2	0.182
ORC-Pump	6.22	0.003
Solar-pump	0.756	0.0004
Total	**1997.2**	**1.0**

6. CONCLUSION

In this study, detailed energy and exergy analysis of the solar driven organic Rankine cycle integrated with parabolic trough solar collectors was conducted. The study considered eight working fluids which includes: o-xylene, ethylbenzene, toluene, dimethylcarbonate (DMC), and benzene, n-Octane, n-nonane and n-heptane. The following can be concluded from this study:

- Increasing the turbine inlet temperature results in increasing the system net electric efficiency, net electric power, and exergy efficiency while it reduces the total exergy destruction rate leading to the improvement in the energetic and exergetic performance of the system.
- The turbine outlet volume flow rate exhibits small decreasing while expansion ratio increases with turbine inlet temperature for all working fluids. The turbine size parameter shows small decreasing with increasing turbine inlet temperature.
- Among the evaluated organic working fluids o-xylene gives the best energetic and exergetic performance while n-heptane delivers the lowest system performance of all working fluids assessed in this study.
- Fluids that delivers low volume flow rate are: n-heptane, DMC (dimethyl carbonate) and benzene, and they are preferable for economic reasons.
- Benzene needs smallest turbine size parameter, while n-nonane requires the largest size parameter of all working fluids.
- The parabolic trough solar collectors are the main source of the exergy destruction resulting in 74.9% of the total exergy loss. This shows that there is a substantial need for a careful design of the PTSC in order to reduce this exergy loss. Next to solar collectors, condenser is another source of exergy destruction where 18% of the total exergy destruction occurs.

NOMENCLATURE

A_{ap}	aperture area (m^2)
A_r	receiver area (m^2)
A_c	receiver cover area (m^2)
Cp	specific heat capacity (kJ/kg)
Cpr	specific heat of heat transfer fluid in the receiver (kJ/kg)
D_o	receiver outer diameter (m)
D_i	receiver inner diameter (m)
D_{co}	receiver cover outer diameter (m)
$\dot{E}_{xd}$	exergy destruction rate (kW)
$\dot{E}_{x,in}$	inlet exergy into the system (kW)
F_R	heat removal factor
F_l	collector efficiency factor
G_b	direct solar irradiation intensity, W/m^2
h	enthalpy (kJ/kg)
h_o	dead state enthalpy (kJ/kg)
hc	convection heat transfer coefficient (W/m^2K)
h_{fi}	convection heat transfer coefficient inside the receiver tube (W/m^2K)
$h_{c,ca}$	convection heat transfer coefficient between ambient and the cover (W/m^2K)
$h_{r,ca}$	radiation heat transfer coefficient between the cover and ambient (W/m^2K)
$h_{r,cr}$	radiation heat transfer coefficient between cover and receiver (W/m^2K)
hr	radiation heat transfer coefficient, (W/m^2K)
IR	irreversibility ratio
k	thermal conductivity of the receiver tube (W/(m. K))
k_{air}	thermal conductivity of the air (W/(m. K))
L	collector module length (m)
$\dot{m}_r$	heat transfer fluid mass flow rate through the receiver (kg/s)
$\dot{m}_f$	mass flow rate of the ORC working fluid (kg/s)
Nt	total number of solar collectors
Nu	Nusselt number
ORC	organic Rankine cycle
P	pressure (kPa)
Pr	Prandtl number

PTC parabolic trough collectors

$\dot{Q}_E$ heat added to the evaporator (kW)

$\dot{Q}_C$ heat rejected by the condenser (kW)

$\dot{Q}_u$ useful energy delivered by collector (kW)

$\dot{Q}_{solar}$ solar radiation that shines up on the collector (kW)

Re Reynolds number

s specific entropy(kJ/kg.K)

s_o dead state specific entropy(kJ/kg.K)

S heat absorbed by the receiver (W/m^2)

T temperature (^{o}C)

T_o dead state temperature (^{o}C)

T_s temperature of the sun (^{o}C)

T_c cover temperature of the receiver (^{o}C)

T_r receiver temperature (^{o}C)

U_o overall heat loss coefficient (kW/K)

U_L solar collector heat loss coefficient between ambient and receiver (kW/K)

w collector width (m)

$\dot{W}_T$ turbine work output (kW)

$\dot{W}_p$ work input to the ORC pump (kW)

$\dot{W}_{net,el}$ net electric power output generated by the solar driven ORC system (kW)

Subscripts

a ambient

ap aperture

b beam

c convection, cover, condenser

cr between cover and reciever

ca between cover and ambient

co cover outer

E evaporator

el electrical

f fluid

fi fluid inside receiver

L loss

o dead state,outer

i inner

p pump

r radiation, receiver

s sun, isentropic

t total

u useful

T Turbine

Greek letters

α absorptance of the receiver

η_r receiver efficiency

η_{exergy} exergy efficiency

$\eta_{,el}$ net electric efficiency

ε_r emittance of the receiver

ε_c emittance of the receiver cover

γ intercept factor

σ Stefan-Boltzman constant (kW/m^{2}K^4)

ρ reflectance of the mirror

τ transmittance of the glass cover

K incidence angle modifier

ψ Physical flow exergy, kJ/kg

ACNOWLEDGEMENT

The authors acknowledge the support provided by the King Saud University Faculty of Engineering research center and Sustainable Energy Technologies Center.

REFERENCES

[1]A. Abu-Zour, S. Riffat Environmental and economic impact of a new type of solar louver thermal collector Int. J. Low Carbon Technol., 1 (3) (2006), pp. 217–227.

[2] WWS Charters. Developing markets for renewable energy technologies. Renewable Energy, 22 (2001), pp. 217–222

[3] K Jagoda, R Lonseth, A Lonseth, T Jackman. Development and commercialization of renewable energy technologies in Canada: an innovation system perspective. Renew Energy, 36 (2011), pp. 1266–1271

[4] PD. Lund. Effects of energy policies on industry expansion in renewable energy, Renewable Energy, 34 (2009), pp. 53–64

[5] JM Cansino, MP Pablo-Romero, R Román, R. Iñiguez. Tax incentives to promote green electricity: an overview of EU-27 countries. Energy Policy, 38 (2010), pp. 6000–6008.

[6] R Sims, HH Rogner, K Gregory. Carbon emission and mitigation cost comparisons between fossil fuel, nuclear and renewable energy resources for electricity generation. Energy Policy, 31 (2003), pp. 1315–1326

[7] TJ Dijkman, RMJ Benders. Comparison of renewable fuels based on their land use using energy densities. Renewable & Sustainable Energy Reviews, 14 (9) (2010), pp. 3148–3155.

[8] Z.H. Yao, Z.F. Wang, Z.W. Lu, X.D. Wei, Modeling and simulation of the pioneer1MW solar thermal central receiver system in China, Renewable Energy 34 (2009) 2437-2446.

[9] X. Li, W.Q. Kong, Z.F. Wang, C. Chang, F.W. Bai, Thermal model and thermodynamic performance of molten salt cavity receiver, Renewable Energy 35 (2010) 981-988.

[10] W. Han, H.G. Jin, J.F. Su, R.M. Lin, Z.F. Wang, Design of the first Chinese 1MW solar-power tower demonstration plant, International Journal of Green Energy 6 (2009) 414-425.

[11] Wei DH, Lu XS, Lu Z, Gu JM. Performance analysis and optimization of organic Rankine cycle (ORC) for waste heat recovery. Energy Conversion Management 2007; 48(4):1113-9).

[12] Roy JP, Misra Ashok. Parametric optimization and performance analysis of a regenerative Organic Rankine Cycle using R-123 for waste heat recovery. Energy 2012; 39: 227-35.

[13] S. Quoilin, M. Orosz, V. Lemort, Modeling and experimental investigation of an organic rankine cycle using scroll expander for small solar applications, in: Proc. Eurosun Conf., Lisbon, Portugal, 7–10 October, 2008.

[14] T. Saitoh, N. Yamada, S. Wakashima, Solar rankine cycle system using scroll expander, Journal of Energy and Engineering 2 (2007) 708–718.

[15] M. Kane, D. Larrain, D. Favrat, Y. Allani, Small hybrid solar power system, Energy 28 (2003) 1427–1443.

[16] W. Yagoub, P. Doherty, S.B. Riffat, Solar energy-gas driven micro-CHP system for an office, Applied Thermal Engineering 26 (2006) 1604–1610.

[17] Ya-Ling He, Dan-Hua Mei, Wen-Quan Tao, Wei-Wei Yang, Huai-Liang Liu. Simulation of the parabolic trough solar energy generation system with Organic Rankine Cycle. Applied Energy .97 (2012) 630–641.

[18] S. Quoilin, M. Orosz, H. Hemond,V. Lemort. Performance and design optimization of a low-cost solar organic Rankine cycle for remote power generation. Solar Energy, 2011;85: 955-966.

[19] Bertrand Fankam Tchanche, George Papadakis, Gregory Lambrinos, Antonios Frangoudakis. Fluid selection for a low-temperature solar organic Rankine cycle. Applied Thermal Engineering 29 (2009) 2468–2476.

[20] Gang Pei, Li Jing, Jie Ji. Analysis of low temperature solar thermal electric generation using regenerative organic Rankine cycle. Appl. Therm. Eng. 2010; 30: 998–1004.

[21] Jing Li, Gang Pei, Jie Ji. Optimization of low temperature solar thermal electric generation with organic Rankine cycle in different areas. Applied Energy 2010; 87 (11):3355-65.

[22] Wang M, Wang J, Zhao Y, Zhao P, Dai Y. Thermodynamic analysis and optimization of a solar-driven regenerative organic Rankine cycle (ORC) based on flat-plate solar collectors. Appl Thermal Eng 2013;50: 816-25.

[23] Fahad A.Al-Sulaiman. Energy and sizing analyses of parabolic trough solar collector integrated with steam and binary vapor cycles. Energy 2013; 58:561-570.

[24] www.Skyfuel.com “Sky Trough @Fact sheet 2011”

[25] Price H, Lüpfert E, Kearney D, Zarza E, Cohen G, Gee R, et al. Advances in parabolic trough solar collectors technology. ASME, J Sol Energy 2002; 124:109-25.

[26] Therminol. Heat transfer fluids by Solutia Inc., Therminol VP-1. www.therminol.com/pages/products/vp-1.asp; Aug. 2012.

[27] Montes MJ, Abanades A, Martinez-Val JM. Performance of a direct steam generation solar thermal power plant for electricity production as a function of the solar multiple. Sol Energy 2009; 83:679-89.

[28] Kalogirou S. Solar energy engineering: processes and systems. Elsevier; 2009.

[29] Duffie J, Beckman W. Solar engineering of thermal processes. John Wiley & Sons, Inc.; 2006.

[30] Yunus A. Cengel, Michael A.Boles. Thermodynamics an engineering Approach.6th edition

[31] Petela R. Exergy analysis of the solar cylindrical-parabolic cooker. Sol Energy 2005; 79 (3):221–33.

[32] Bejan A, Tsatsaronis G, Moran M. Thermal design and optimization. John Wiley and Sons, Inc.; 1996.

[33] Macchi E, Perdichizzi A. Efficiency prediction for axial-flow turbines operating with non-conventional fluids. Transaction of the ASME, Journal of Engineering for Power 1981; 103:718-24.

[34] EES. Engineering equation solver. Available online: http://www.mhhe.com/engcs/mech/ees/whatisees.html (accessed on 17 February 2012).

[35] Madhawa Hettiarachchi HD, Golubovic M, Worek WM, Ikegami Y. Optimum design criteria for an Organic Rankine cycle using low-temperature geothermal heat sources. Energy 2007; 32(9): 1698–1706.